Cancer Science
Japanese Cancer Association JCA
Open Access

Cytochrome c1 in ductal carcinoma *in situ* of breast associated with proliferation and comedo necrosis

Mayuko Chishiki,[1] Kiyoshi Takagi,[1] Ai Sato,[1] Yasuhiro Miki,[2,3] Yuta Yamamoto,[1] Akiko Ebata,[4,5] Yukiko Shibahara,[2] Mika Watanabe,[6] Takanori Ishida,[4] Hironobu Sasano[2,6] and Takashi Suzuki[1]

Departments of [1]Pathology and Histotechnology, Tohoku University Graduate School of Medicine; [2]Anatomic Pathology, Tohoku University Graduate School of Medicine, Sendai; [4]Breast and Endocrine Surgical Oncology, Tohoku University Graduate School of Medicine; [3]Department of Disaster Obstetrics and Gynecology, International Research Institute of Disaster Science, Tohoku University, Sendai; [5]Department of Surgery Osaki Citizen Hospital, Osaki; [6]Department of Pathology Tohoku University Hospital, Sendai, Japan

Key words

Comedo necrosis, CYC1, DCIS, immunohistochemistry, proliferation

Correspondence

Takashi Suzuki, Department of Pathology and Histotechnology, Tohoku University Graduate School of Medicine, 2-1 Seiryo-machi, Aoba-ku, Sendai, Miyagi-ken, 980-8575 Japan.
Tel/Fax: +81-22-717-7947;
E-mail: t-suzuki@patholo2.med.tohoku.ac.jp

Funding Information
None declared.

Received November 4, 2016; Revised March 9, 2017; Accepted April 4, 2017

Cancer Sci **108** (2017) 1510–1519

doi: 10.1111/cas.13251

It is well known that comedo necrosis is closely associated with an aggressive phenotype of ductal carcinoma *in situ* (DCIS) of human breast, but its molecular mechanisms remain largely unclear. Therefore, in this study, we first examined the gene expression profile of comedo DCIS based on microarray data and identified *CYC1* as a gene associated with comedo necrosis. Cytochrome c1 (CYC1) is a subunit of complex III in the mitochondrial oxidative phosphorylation that is involved in energy production. However, the significance of CYC1 has not yet been examined in DCIS. We therefore immunolocalized CYC1 in 47 DCIS cases. CYC1 immunoreactivity was detected in 40% of DCIS cases, and the immunohistochemical CYC1 status was significantly associated with tumor size, nuclear grade, comedo necrosis, van Nuys classification, and Ki-67 labeling index. Subsequent *in vitro* studies indicated that CYC1 was significantly associated with mitochondrial membrane potential in MCF10DCIS.com DCIS cells. Moreover, CYC1 significantly promoted proliferation activity of MCF10DCIS.com cells and the cells transfected with CYC1 siRNA decreased pro-apoptotic caspase 3 activity under hypoxic or anoxic conditions. Considering that the center of DCIS is poorly oxygenated, these results indicate that CYC1 plays important roles in cell proliferation and comedo necrosis through the elevated oxidative phosphorylation activity in human DCIS.

Breast cancer is the most common malignant neoplasm in women worldwide. Among these, the incidence of DCIS has been markedly increasing during the past two decades, and now accounts for >20% of all breast cancer diagnoses.[1] Ductal carcinoma *in situ* is generally considered a precursor lesion of invasive ductal carcinoma;[2] it is very important to examine the biological features of DCIS to improve clinical outcomes for breast cancer patients.

Ductal carcinoma *in situ* encompasses a wide spectrum of diseases ranging from low-grade lesions that are not life threatening to high-grade lesions. It is typically classified according to architectural pattern (e.g., solid, cribriform, papillary), grade of nuclear atypia, and presence or absence of comedo necrosis that exists in the center of DCIS lesion with calcification.[3] Comedo necrosis is reportedly associated with higher proliferation activity[4] and clinically aggressive behavior,[5] and it is considered an important factor predicting local recurrence after surgical treatment in DCIS patients.[6,7] Comedo necrosis can be easily recognized in clinical practice, but the occurring mechanism remains largely unknown. Therefore, in this study, we studied the gene expression profile of comedo DCIS based on microarray data and identified *CYC1* as a gene closely associated with comedo necrosis.

It is well known that mitochondria are indispensable for energy metabolism. Approximately 90% of cellular ATP is generated in mitochondria through the OXPHOS pathway,[8] and CYC1 (also referred to cytochrome c1) is a heme-containing subunit of complex III. Overexpression of CYC1 mRNA has been reported in human osteosarcoma and nasopharyngeal carcinoma,[9,10] and very recently Han *et al.*[11] reported that CYC1 immunoreactivity was increased in breast carcinoma compared to the benign mass. However, the significance of CYC1 has not been known in DCIS to the best of our knowledge. Therefore, we examined CYC1 in DCIS using immunohistochemistry and *in vitro* studies to explore its clinical and biological significance.

Materials and Methods

Patients and tissues. Two sets of tissue specimens were evaluated in this study. The first set consisted of four specimens of ER-positive pure DCIS (two comedo DCIS and two non-comedo DCIS cases) obtained from Japanese female patients (age range, 51–77 years) who underwent surgical treatment between 2003 and 2008 in the Department of Surgery, Tohoku University Hospital (Sendai, Japan). These specimens were stored at −80°C for subsequent microarray analysis.

As a second set, 47 specimens of pure DCIS were obtained from Japanese female patients (age range, 39–80 years) who underwent surgical treatment between 1998 and 2005 in the

Department of Surgery, Tohoku University Hospital. All specimens had been fixed in 10% formalin and embedded in paraffin wax. The tumor size was histologically evaluated in 39 cases. Nuclear grade[12] and van Nuys classification[6] were determined according to previous reports. The mean follow-up time after surgery was 46 months (range, 8–104 months) in this study, and no patients had recurrent disease or died within the duration.

The research protocol was approved by the Ethics Committee at Tohoku University School of Medicine.

Laser capture microdissection/microarray analysis. Gene expression profiles of ER-positive pure DCIS were examined using microarray analysis, and these were assembled previously.[13] Briefly, DCIS cells were dissected under the light microscope and laser transferred from these frozen sections. Whole Human Genome Oligo Microarray (G4112F; ID: 012391; Agilent Technologies, Waldbronn, Germany), containing 41 000 unique probes, was used in this study, and sample preparation and processing were carried out according to the manufacturer's protocol. The relative levels of gene expression were calculated by global normalization, and scatter plot and GO analyses of the microarray data were carried out using GeneSpring 12.6.1 (Agilent Technologies).

Immunohistochemistry. Rabbit polyclonal antibody for CYC1 (PA5-25257) and mouse mAb for Ki-67 (MIB1) were purchased from Thermo Fisher Scientific (Waltham, MA, USA) and Dako (Carpinteria, CA, USA), respectively. The antigen–antibody complex was visualized with DAB solution and counterstained with hematoxylin. We used human tissue of the stomach as a positive control based on a data sheet of CYC1 antibody by Novus Biologicals (http://www.novusbio.com/CYC1-Antibody_NBP1-86872.html#dsTab0) and normal rabbit IgG instead of the primary antibody as a negative control for CYC1 immunostaining in this study.

Immunohistochemistry for ER (CONFIRM anti-ER [SP1]; Roche Diagnostics Japan, Tokyo, Japan) and PR (CONFIRM anti-PR [1E2]; Roche Diagnostics Japan) was carried out with Ventana Benchmark XT (Roche Diagnostics Japan), and that for HER2 was carried out using HercepTest (Dako).

Scoring of immunoreactivity. CYC1 was immunolocalized in the cytoplasm of carcinoma cells, and weakly present in the epithelium of non-neoplastic mammary glands. We evaluated CYC1-positive carcinoma cells if the CYC1 immunoreactivity was stronger compared to the non-neoplastic mammary glands. Cases that had more than 10% positive carcinoma cells were considered positive for CYC1 status, as the 10% cut-off value is frequently used as a reproducible evaluation of various cytoplasmic immunostaining.[14,15] Immunoreactivity for ER, PR, and Ki-67 was detected in the nucleus, and the percentage of immunoreactivity (labeling index; LI) was determined. Cases with ER LI >1% were considered ER-positive breast carcinoma according to a previous report.[16] HER2 immunoreactivity was evaluated according to the grading system proposed in HercepTest (Dako).

Cell line. The MCF10DCIS.com DCIS cell line was purchased from Asterand (Detroit, MI, USA), and cultured in RPMI-1640 (Sigma-Aldrich, St.Louis, MO, USA) containing 10% FBS (Thermo Fisher Scientific). MCF10DCIS.com cells generated basal-type lesions and formed comedo DCIS in a mouse transplantation model.[17,18]

Small interfering RNA transfection. Two siRNA oligonucleotides for siCYC1 used in this study were designed as follows: siCYC1-1 (sense, 5′-rGrCUrGUUrCrGrArCUrAUUUrCrCrCrATT-3′; antisense, 5′-UrGrGrGrArArAUrArGUrCrGrArArCrArGrCTT-3′) and siCYC1-2 (sense, 5′-rGUrCrArCUrGrCrGrGrGrArArGrGUrCUrCTT-3′; antisense, 5′-rGrArGrArCrCUUrCrCrCrGrCrArGUrGrArCTT-3′). These were purchased from Sigma-Aldrich. MISSION siRNA Universal Negative Control (Sigma-Aldrich) was used as siCTRL. The siRNAs were transfected using the Lipofectamine 3000 Reagent (Invitrogen, Carlsbad, CA, USA) according to the manufacturer's protocol.

Plasmid transfection. The CYC1 expression plasmid was constructed by inserting a full-length ORF of human CYC1 mRNA (NM_001916) into pBApo-CMV Pur vector (Takara Bio, Otsu, Japan) using the restriction enzymes *Bam*HI and *Hind*III (CYC1 plasmid). The plasmid was transfected into MCF10DCIS.com cells using Lipofectamine 3000 Reagent (Invitrogen). As a control, empty vector pcDNA3.1(−) was transfected in this study.

Real-time PCR. Total RNA was extracted using TRI Reagent (Molecular Research Center, Cincinnati, OH, USA), and cDNA was synthesized using a ReverTra Ace qPCR RT Master Mix with gDNA Remover (Toyobo, Osaka, Japan). Real-Time PCR was carried out using the THUNDERBIRD SYBR qPCR Mix (Toyobo). The primer sequences of CYC1 and RPL13A were: CYC1 (NM_001916), 5′-GAGGTGGAGGTTCAAGACGG-3′ (forward) and 5′-TAGCTCGCACGATGTAGCTG-3′ (reverse)[19]; and RPL13A (NM_012423), 5′-CCTGGAGGAGAAGAGGAAAGAGA-3′ (forward) and 5′-TTGAGGACCTCTGTGTATTTGTCAA-3′ (reverse). The CYC1 mRNA level was calculated as the ratio of the RPL13A mRNA level in this study.

Immunoblotting. The mitochondrial protein from MCF10DCIS.com cells was extracted according to a previous report[20] and M-PER (Thermo Fisher Scientific Pierce Biotechnology, Rockford, IL, USA). The lysate proteins (2 μg) were subjected to SDS–PAGE (10% acrylamide gel) and transferred onto Hybond PVDF membranes (GE Healthcare, Little Chalfont, UK). The primary anti-CYC1 antibody used was the same as that in the immunohistochemistry. Antimitochondrial voltage-dependent anion channel 1 antibody (sc-390996; Santa Cruz Biotechnology, Dallas, TX, USA) was also used as an internal control for mitochondrial protein.[21]

Measurement of mitochondrial membrane potential. Mitochondrial potential was analyzed using a JC-1 Mitochondrial Membrane Potential Assay Kit (Cayman Chemical, Ann Arbor, MI, USA). After staining, flow cytometric analysis was undertaken acquiring FL1 (green; JC-1 monomers) and FL2 (red; JC-1 aggregates) signals using a fluorescence microscope (FSX100; Olympus, Tokyo, Japan).

Cell proliferation assay and caspase 3 activity assay under hypoxic conditions. The cell proliferation status was measured by the WST-8 method using Cell Counting Kit-8 (Dojindo Molecular Technologies, Kumamoto, Japan) 4 days after the transfection in these cells. Hypoxic (10% 0_2) and anoxic (0% 0_2) conditions were generated using an Anaeropack (Mitsubishi Gas Chemicals, Tokyo, Japan). Pro-apoptotic caspase 3 activity was evaluated using a CaspGLOW Fluorescein Active Caspase-3 Staining Kit (BioVision, Milpitas, CA, USA). The luminescence of each sample in a plate-reading luminometer was measured as directed by the luminometer manufacturer (PHERAstar FS; BMG LABTECH JAPAN, Saitama, Japan).

Statistical analysis. Immunohistochemical CYC1 status and clinicopathologic factors were evaluated by Student's *t*-test or a cross-table using the χ^2-test. In the *in vitro* experiments, the statistical analyses were carried out using Student's *t*-test and Fisher's PLSD test. The statistical analyses were undertaken using StatView 5.0J software (SAS Institute, Cary, NC, USA), and $P < 0.05$ was considered significant in this study.

Results

Gene expression profile in comedo DCIS. We first examined gene expression profiles of DCIS cells according to the status of comedo necrosis by microarray analysis. In this analysis, when the expression ratio of a gene in the comedo DCIS group compared to that in the non-comedo group was >2.0 or <0.5, we determined that the gene was predominantly expressed in the comedo or non-comedo group respectively, according to the cut-off value previously used.[22] As shown in Figure 1(a), a scatter plot revealed that 2871 genes (7%) were predominantly expressed in the comedo type (group A; comedo DCIS/non-comedo DCIS ratio >2.0), 1750 genes (4%) were mainly expressed in the non-comedo type (group B; ratio <0.5), and 36 472 genes (89%) had a similar expression level in both groups (group C; ratio 0.5–2.0).

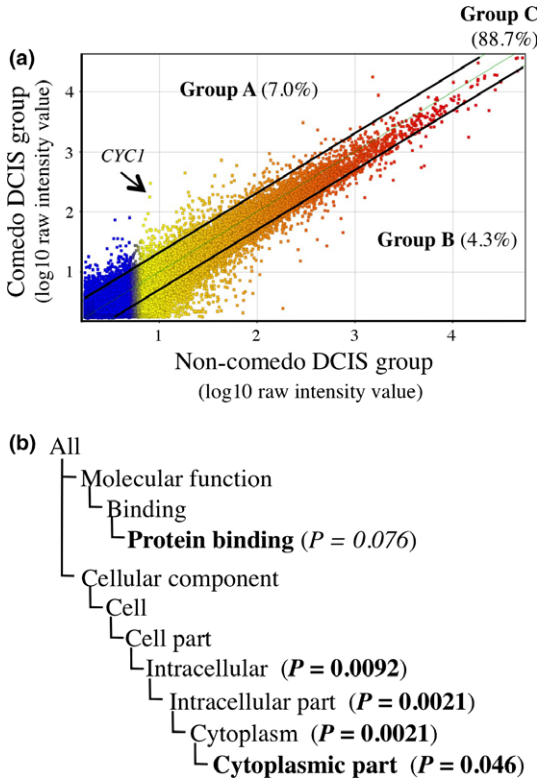

Fig. 1. Gene expression profile in comedo ductal carcinoma *in situ* (DCIS). (a) Scatter plot analysis of microarray data of DCIS according to the status of comedo necrosis (n = 2 each group), in which 41 093 genes were plotted on the logarithmic graph. Those genes that were more than 2.0-fold higher in the comedo DCIS group or non-comedo DCIS group were located outside of the diagonal line, and classified as group A or group B, respectively. Genes with ≤2.0-fold change were classified as group C. Arrow, location of cytochrome c1 (CYC1). (b) Gene ontology (GO) terms enriched in the comedo DCIS group compared to all the DCIS cases in group A genes by GO analysis. *P*-value <0.05 and 0.05 ≤ *P*-value < 0.10 were considered significant and marginally significant, respectively. GO terms are summarized. Bold, GO terms whose gene lists are summarized in Table 1. *P*-values are summarized following the Gene Ontology Consortium (http://geneontology.org/page/go-enrichment-analysis). *P*-values indicate the probability or chance of seeing at least x number of genes out of the total n genes in the list annotated to a particular GO term, given the proportion of genes in the whole genome that were annotated to that GO term. The closer the *P*-value is to zero, the more significant the particular GO term associated with the group of genes (i.e., the less likely the observed annotation of the particular GO term to a group of genes occurred by chance).

When we undertook GO analysis in group A genes, "intracellular" (P = 0.0092), "intracellular part" (P = 0.0021), "cytoplasm" (P = 0.0021) and "cytoplasmic part" (P = 0.046) were identified as significantly enriched GO terms in comedo DCIS compared to all the DCIS cases, and "protein binding" (P = 0.075) was marginally significant (Fig. 1b). The definitions of these GO terms are summarized in Table S1. As shown in Table 1, *CYC1* showed the highest increase (31-fold) among the genes in the "cytoplasmic part", indicating its possible involvement in comedo necrosis. *S100A8* showed the highest increase (34-fold) among the genes in "protein binding," which was a marginally enriched GO term in comedo DCIS in this study. The known functions of these genes are briefly described in Table S2.

CYC1 immunolocalization in human DCIS. Immunoreactivity of CYC1 was detected in the cytoplasm of carcinoma cells in DCIS tissues (Fig. 2a–c). CYC1 was also weakly present in the cytoplasm of epithelial cells in non-neoplastic glands, but it was negative in the stroma (Fig. 2d). In the positive control, CYC1 was immunolocalized in the epithelium of the fundic glands in the stomach (Fig. 2e,f).

Associations between immunohistochemical CYC1 status and clinicopathologic parameters in DCIS are shown in Table 2. When DCIS cases showed stronger CYC1 immunointensity compared with the non-neoplastic mammary gland, it was considered positive for CYC1 status. The number of CYC1-positive DCIS was 19 of 47 (40%) cases examined. The CYC1 status was significantly associated with tumor size (P = 0.048), nuclear grade (P = 0.032), comedo necrosis (P = 0.0065), van Nuys classification (P = 0.0021), and Ki-67 LI (P = 0.011). No significant association was detected between CYC1 status and patient age, menopausal status, ER status, PR LI, or HER2 status in this study.

We could not examine the association between CYC1 status and prognosis of DCIS patients in this study, because no patients had recurrent disease or died within the follow-up duration after surgery.

Association between CYC1 expression and mitochondrial membrane potential in DCIS cells. In this study, microarray data identified *CYC1* as a gene associated with comedo necrosis in ER-positive DCIS, and the following immunohistochemical analysis showed CYC1 immunoreactivity was detected in DCIS tissues regardless of the ER status. To further evaluate the biological functions of CYC1 in human breast DCIS cells, we next transfected specific siRNA for CYC1 in ER-negative MCF10DCIS.com cells, because no ER-positive DCIS cells were available to the best of our knowledge. The mRNA expression level of CYC1 was significantly decreased in cells transfected with siCYC1-1 (Fig. 3a, upper panel) and siCYC1-2 (Fig. 3b, upper panel) in a dose-dependent manner at 3 days after transfection compared with those in cells transfected with siCTRL (10 nM). When the cells were transfected with 10 nM siRNA, the ratio of CYC1 mRNA level to the control level and its P-value were 30% and $P < 0.001$ (siCYC1-1), and 39% and $P < 0.001$ (siCYC1-2). The mitochondrial protein levels of CYC1 were also markedly decreased in cells transfected with CYC1 siRNA compared with those in the control cells under the same conditions (Fig. 3a,b, lower panels).

JC-1 produces two fluorescence emission peaks. The JC-1 monomer, which is the predominant form at low mitochondrial membrane potential, emits green fluorescence, and the JC-1 aggregates, the predominant species at high mitochondrial membrane potential, emit red fluorescence. When we carried out the JC-1 assay, green fluorescence was predominantly

detected in MCF10DCIS.com cells transfected with siCYC1-1 (Fig. 3c) and siCYC1-2 (Fig. 3d), whereas red fluorescence was mainly detected in MCF10DCIS.com cells transfected with siCTRL, in the merged image. The red/green ratio, which reflects mitochondrial membrane potential,[23] was significantly lower in cells transfected with siCYC1-1 (27%, $P < 0.001$) and siCYC1-2 (49%, $P < 0.001$). These results suggest that CYC1 is associated with mitochondrial membrane potential in MCF10DCIS.com cells.

Table 1. Top 10 genes in "cytoplasmic part" ($P = 0.046$) and "protein binding" ($P = 0.075$) in gene ontology analysis of comedo and non-comedo ductal carcinoma *in situ* (DCIS) tissue

Cytoplasmic part		Protein binding	
Fold	Gene symbol	Fold	Gene symbol
31.2	**CYC1**	33.7	*S100A8*
15.2	*S100A7*	15.2	*S100A7*
13.4	KCNA5	14.6	WISP2
12.2	KCNK1	14.6	GSTM3
11.7	PLEK	13.5	*CD24*
9.55	HSD17B1	13.4	KCNA5
9.19	CX3CL1	11.8	MET
8.73	PTN	11.7	PLEK
8.31	CYB5R2	9.34	IGFBP7
7.98	CXCR4	9.22	*S100A9*

Bold text indicates a gene identified by immunohistochemistry. Italic text shows genes described in the Discussion section. Fold, expression ratio in comedo DCIS group to that in non-comedo DCIS group.

Effects of CYC1 on cell proliferation and caspase 3 activity under hypoxia in DCIS cells. As CYC1 status was significantly associated with Ki-67 LI in DCIS tissues in this study, we next examined the effects of CYC1 expression on cell proliferation in MCF10DCIS.com cells. As shown in Figure 4(a,b), the number of cells transfected with CYC1 siRNA was dose-dependently decreased compared to that of the control cells transfected with siCTRL cells 4 days after transfection (10 nM; 63% and $P < 0.001$ for siCYC1-1 and 59% and $P < 0.001$ for siCYC1-2).

Our immunohistochemical analysis also indicated that CYC1 status was significantly associated with comedo necrosis, suggesting that CYC1 is involved in apoptosis under hypoxic conditions because the center of DCIS is poorly oxygenated.[24] Proliferation activity was significantly increased in MCF10DCIS.com cells transfected with siCYC1-1 cells under hypoxia or anoxia for 2 days (1.1-fold and $P < 0.05$ under hypoxia; 1.2-fold and $P < 0.001$ under anoxia), whereas it was not significant in MCF10DCIS.com cells transfected with siCYC1-2 cells under the same conditions (Fig. 4d,e). On the contrary, as shown in Figure 4(e), caspase 3 activity was significantly decreased in MCF10DCIS.com cells transfected with siCYC1-1 cells when these cells were incubated under hypoxic

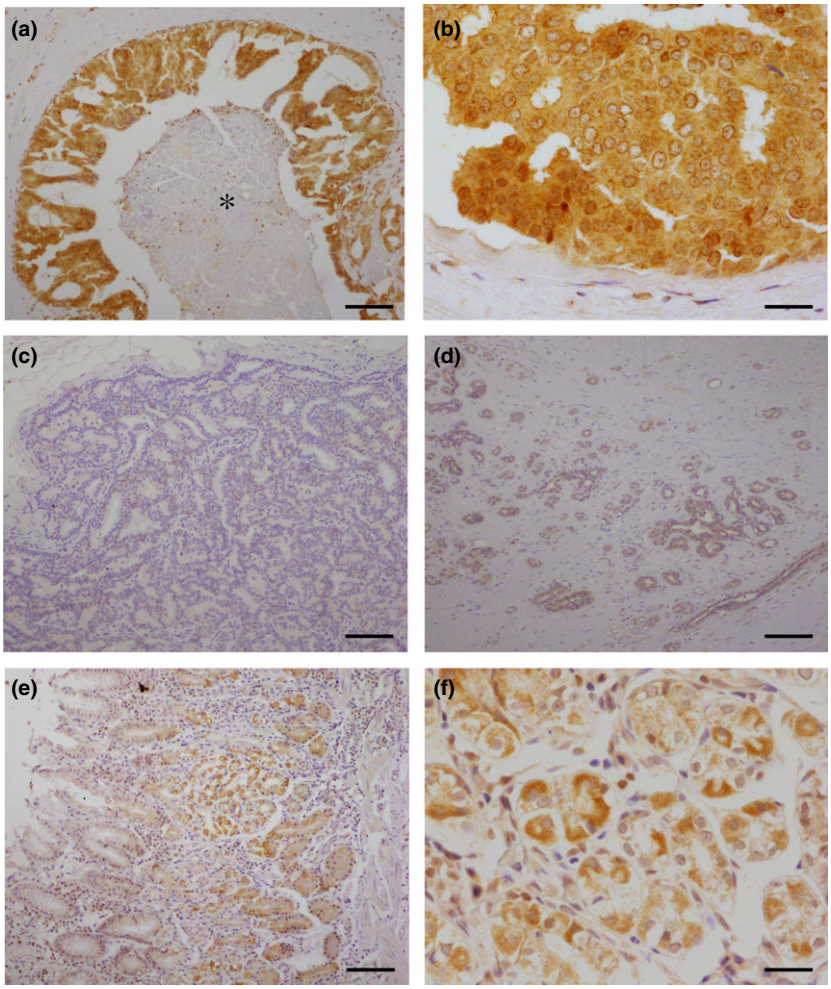

Fig. 2. Immunohistochemistry for cytochrome c1 (CYC1) in ductal carcinoma *in situ* (DCIS). (a,b) Higher magnification, CYC1 was immunolocalized in the cytoplasm of DCIS cells. *Comedo necrosis. (c) CYC1-negative DCIS case. (d) CYC1 immoreactivity was weakly observed in the morphologically normal mammary gland. (e,f) Higher magnification, in a positive control section, CYC1 immunoreactivity was detected in the fundic glands of the stomach. Bar = 100 μm (a,c–f) or 400 μm (b,f).

Table 2. Association between immunohistochemical cytochrome c1 (CYC1) status and clinicopathological parameters in 47 cases of ductal carcinoma *in situ*

	CYC1 status		*P*-value
	+ (n = 19)	− (n = 28)	
Age, years†	60.3 ± 2.5	58.9 ± 1.7	0.650
Menopausal status			
Premenopausal	3	6	
Postmenopausal	16	22	0.630
Tumor size, cm†	4.0 ± 0.6	2.7 ± 0.3	**0.048**
Nuclear grade			
1 + 2	12	25	
3	7	3	**0.032**
Comedo necrosis			
Present	17	15	
Absent	2	13	**0.007**
van Nuys classification			
1	0	12	
2	12	13	
3	7	3	**0.002**
ER status			
Positive	18	26	
Negative	1	2	0.800
PR LI, %†‡	49.8 ± 7.4	44.0 ± 6.1	0.550
HER2 status			
Positive	10	9	
Negative	9	19	0.160
Ki-67 LI, %†	6.5 ± 0.8	4.1 ± 0.6	**0.011**

†Data are presented as mean ± SEM. All other values represent the number of cases. ‡Three estrogen receptor (ER)-negative cases were excluded. Statistical analysis was evaluated by Student's *t*-test or a cross-table using the χ^2-test. $P < 0.05$ were considered significant (shown in bold). HER2, human epidermal growth factor receptor 2; LI, labeling index; PR, progesterone receptor.

and anoxic conditions (53% and $P < 0.01$ under hypoxia; 46% and $P < 0.01$ under anoxia). Similar tendency was also detected in the cells transfected with siCYC1-2, although *P*-values did not reach significance (Fig. 4f).

We next transfected CYC1 plasmid in MCF10DCIS.com cells. As shown in Figure 5, CYC1 expression level was markedly increased both at mRNA (22-fold and $P < 0.01$) (Fig. 5a, upper panels) and protein (Fig. 5a, lower panels) levels; however, the mitochondrial membrane potential (1.03-fold and $P = 0.44$) (Fig. 5b) and cell proliferation activity (1.1-fold and $P = 0.26$) (Fig. 5c) were not significantly changed. Cell proliferation activity was similar level in MCF10DCIS.com cells transfected with CYC1 plasmid regardless of the oxygen level (Fig. 5d), while the caspase 3 activity was decreased (82% and $P < 0.05$ under hypoxia; 77% and $P < 0.05$ under anoxia) (Fig. 5e).

Discussion

Gene expression profiling is a very important method to survey molecular features of a selective group of breast carcinoma[13,25] in addition to conventional clinical and histopathologic examinations. This is the first study to show gene expression profiles of comedo DCIS. Results of our microarray analysis did reveal that "cytoplasmic part" and "protein binding" were enriched GO terms in comedo DCIS. Among these genes (Table 1), *S100A7* (psoriasin), which is a member of the S100 family of calcium-binding proteins, and *CD24* were linked and related to the differentiation of mammary epithelial cells.[26] S100A7 was expressed in DCIS at the highest levels and it is involved in the transition to invasive breast carcinoma.[27] S100A8 (calgranulin A) and S100A9 (calgranulin B), also members of the S100 family, have been shown to be highly expressed in DCIS,[28] and play important roles in growth, invasion, and metastasis in breast cancer cells.[29] Muggerud *et al.*[25] identified a subgroup of high-grade DCIS that show a distinctive gene expression profile compared to other DCIS and an invasive-like phenotype by microarray analysis. S100A8 was highly expressed in this subgroup. Taken together with these previous reports and our present results, comedo DCIS is suggested to show aggressive molecular features. *CYC1* showed the highest expression ratio in genes of "cytoplasmic part," a significantly enriched GO term in comedo DCIS (Table 1), but its significance has not yet been established in DCIS to the best of our knowledge.

This is the first study to reveal the clinical significance of CYC1 in DCIS. In this study, CYC1 immunoreactivity was detected in 40% of DCIS cases, whereas it was very weak in the non-neoplastic epithelium. The CYC1 status was significantly associated with nuclear atypia, comedo necrosis, and van Nuys classification in the DCIS cases. The van Nuys classification was reported to be significantly associated with local recurrence of DCIS, and it has been established as a potent prognostic classification for DCIS patients.[6] Previously, Fang *et al.*[9] found that CYC1 expression was upregulated in nasopharyngeal carcinomas compared to non-cancerous nasopharyngeal tissues by microarray analysis, and Li *et al.*[10] reported that CYC1 was overexpressed in human osteosarcoma tissues and cell lines. Moreover, Han *et al.*[11] very recently reported that CYC1 immunoreactivity was significantly increased in breast carcinoma compared to benign breast tumors. Our present results are consistent with these previous reports, and it is suggested that CYC1 expression is increased in an aggressive phenotype of DCIS compared to normal breast tissue.

Expression of CYC1 is induced by oxygen and repressed by glucose.[30] Ivanova *et al.*[31] reported that CYC1 expression was stimulated by estrogen through nuclear respiratory factor 1 in MCF-7 breast carcinoma cells. However, considering that CYC1 immunoreactivity was relatively widely detected in DCIS tissues, CYC1 expression may be induced in the process of breast carcinogenesis by other factors such as oncogenes. Limited information is available about the regulatory mechanisms of CYC1 expression, and further examination is required.

In our present study, CYC1 immunoreactivity was significantly associated with Ki-67 LI in DCIS tissues. Ki-67 antibody recognizes cells in all phases of the cell cycle except G_0 (resting) phase, and Ki-67 LI is well correlated with proliferation activity of breast carcinoma.[32] In addition, results of *in vitro* studies showed that MCF10DCIS.com cells transfected with siRNA against CYC1 significantly decreased the cell proliferation, although ER-positive DCIS cells were not available for our *in vitro* experiments. Previously, Li *et al.*[10] reported that CYC1 silencing by shRNA transfection inhibited proliferation activity of osteosarcoma cells *in vitro* and suppressed tumor growth in a mouse xenograft model *in vivo*. Han *et al.*[11] also showed that silencing CYC1 suppressed proliferation of invasive breast carcinoma cells (MDA-MB-231), consistent with our present results. Our *in vitro* experiments

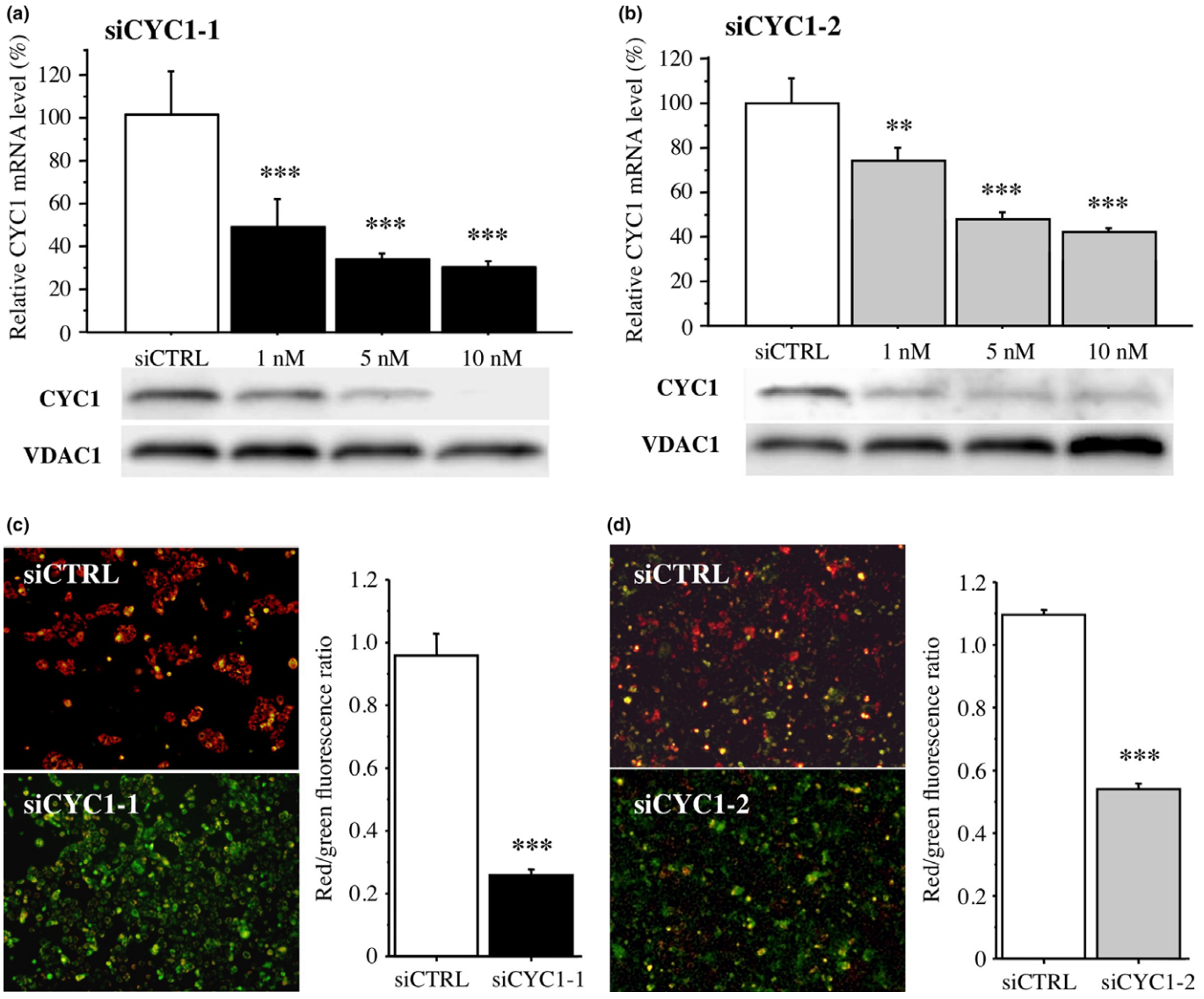

Fig. 3. Effects of cytochrome c1 (CYC1) on mitochondrial membrane potential in MCF10DCIS.com ductal carcinoma *in situ* cells. (a,b) Upper panel shows expression of CYC1 mRNA in MCF10DCIS.com cells transfected with CYC1-specific siRNA (siCYC1-1 [a, closed bar] and siCYC1-2 [b, gray bar]) or negative control siRNA (siCTRL, open bar) by real-time PCR. Lower panel shows the corresponding CYC1 immunoreactivity by immunoblotting. Voltage-dependent anion channel 1 (VDAC1) immunoreactivity is shown as an internal control of mitochondrial protein. (c,d) JC-1 assays in MCF10DCIS.com cells transfected with siCYC1-1 (c; 10 nM, closed bar) and siCYC1-2 (d; 10 nM, gray bar) or siCTRL (open bar). Left panels show representative merged images. Green fluorescence shows JC-1 monomer (low mitochondrial membrane potential) and red fluorescence represents JC-1 aggregate (high mitochondrial membrane potential); cells show yellow if both fluorescence are similar levels. Right panels show their red/green fluorescence ratio. Data are presented as mean ± SD ($n = 3$). Statistical analyses were carried out using Student's *t*-test and Fisher's PLSD test. $^{**}P < 0.01$; $^{***}P < 0.001$ versus control cells transfected with siCTRL (left open bar).

revealed that CYC1 expression levels reflected mitochondrial membrane potential in MCF10DCIS.com cells, and Owens *et al.*[33] reported that immunoreactivity of UQCRFS1/RISP, which is another subunit of complex III in mitochondrial OXPHOS, was increased in DCIS compared to benign breast tissue. Therefore, it is suggested that CYC1 plays an important role in the cell proliferation of DCIS, possibly through elevated OXPHOS activity.

Although CYC1 is an important subunit of mitochondria complex III,[11] MCF10DCIS.com cells transfected with CYC1 plasmid did not significantly increase mitochondrial membrane potential or cell proliferation activity (Fig. 5b,c) in this study. Considering that CYC1 was abundantly expressed in MCF10DCIS.com cells, as shown in Figure 3(a,b), forcibly expressed CYC1 might not cause further increment of OXPHOS activity in MCF10DCIS.com cells.

It is known that proliferating carcinoma cells preferentially use anaerobic glycolysis rather than OXPHOS for energy production, and the metabolic alteration is commonly referred to as the Warburg effect.[34] Although efficiency of ATP synthesis in aerobic glycolysis is much lower compared to OXPHOS, the glycolytic pathway can provide precursors for biomolecules necessary for proliferation.[8,35] Indeed, Sato-Tadano *et al.*[15] showed that immunoreactivity of hexokinase II, which is involved in the rate-limiting step of glycolysis, was detected in 44% of invasive breast carcinomas and it was a potent worse prognostic factor. However, both OXPHOS and glycolysis are active inside tumor cells at various rates; for instance, the

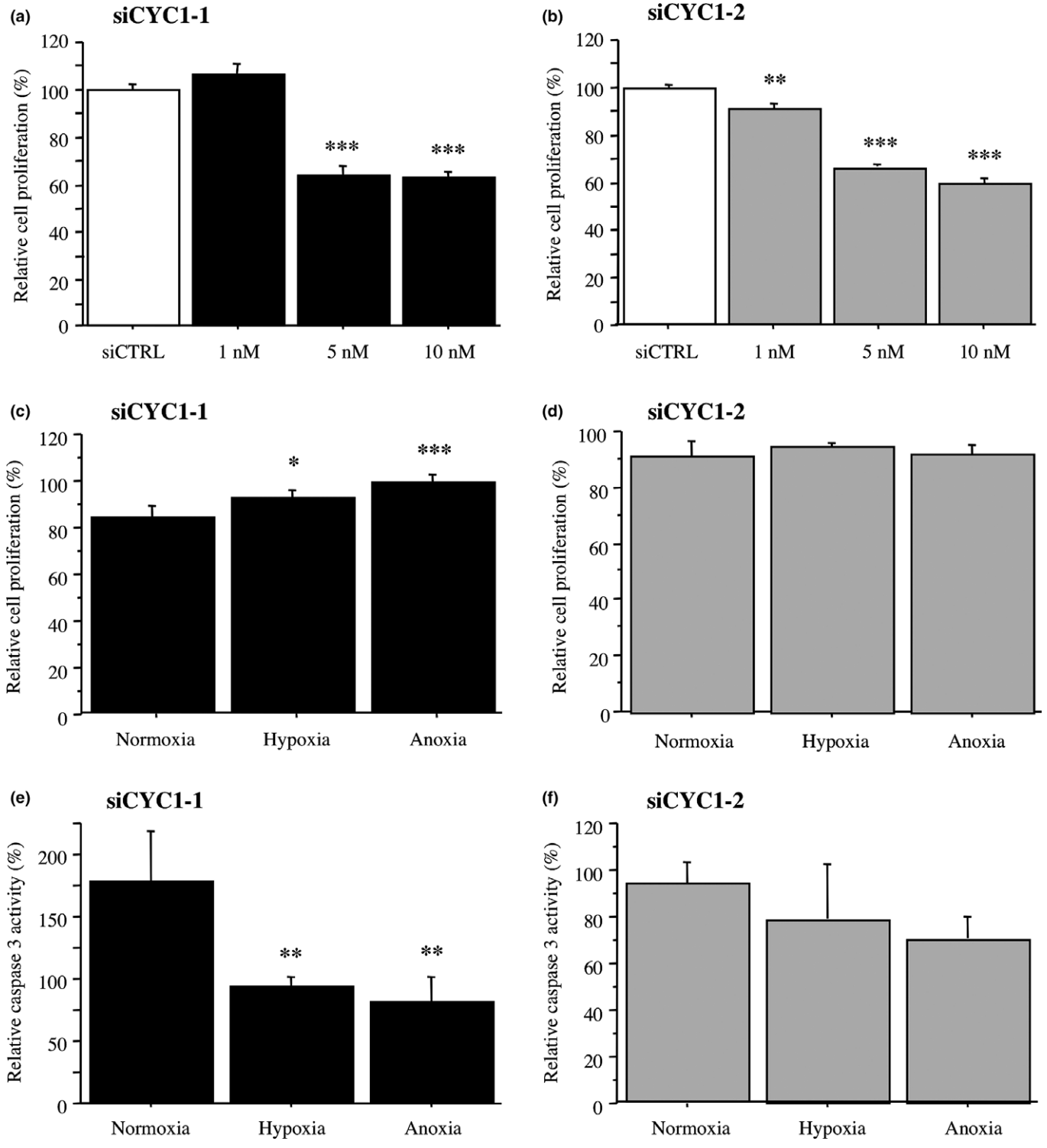

Fig. 4. Effects of cytochrome c1 (CYC1) knockdown on cell proliferation and caspase 3 activity under hypoxia in MCF10DCIS.com ductal carcinoma *in situ* cells. (a,b) WST-8 assay in MCF10DCIS.com cells transfected with siCYC1-1 (a, closed bar), siCYC1-2 (b, gray bar), or negative control siRNA (siCTRL; open bar). Relative proliferative activity of these cells was summarized as a ratio (%) compared to the control cells transfected with siCTRL at 4 days after treatment (left open bar). (c,d) WST-8 assay in MCF10DCIS.com cells transfected with siCYC1-1 (10 nM) (c) or siCYC1-2 (10 nM) (d) under normoxia, hypoxia, or anoxia for 2 days. Relative cell proliferation activity was evaluated as a ratio (%) compared to the mean value of control cells transfected with siCTRL under the same conditions. (e,f) Caspase 3 activity assays in MCF10DCIS.com cells transfected with siCYC1-1 (10 nM) (e) or siCYC1-2 (10 nM) (f). Cells were incubated under the indicated conditions for 5 h. Relative caspase 3 activity was evaluated as a ratio (%) compared to the mean value of control cells transfected with siCTRL under the same condition. Data were presented as the mean ± SD ($n = 3$). Statistical analyses were carried out using Fisher's PLSD test. *$P < 0.05$; **$P < 0.01$; ***$P < 0.001$ versus left bar.

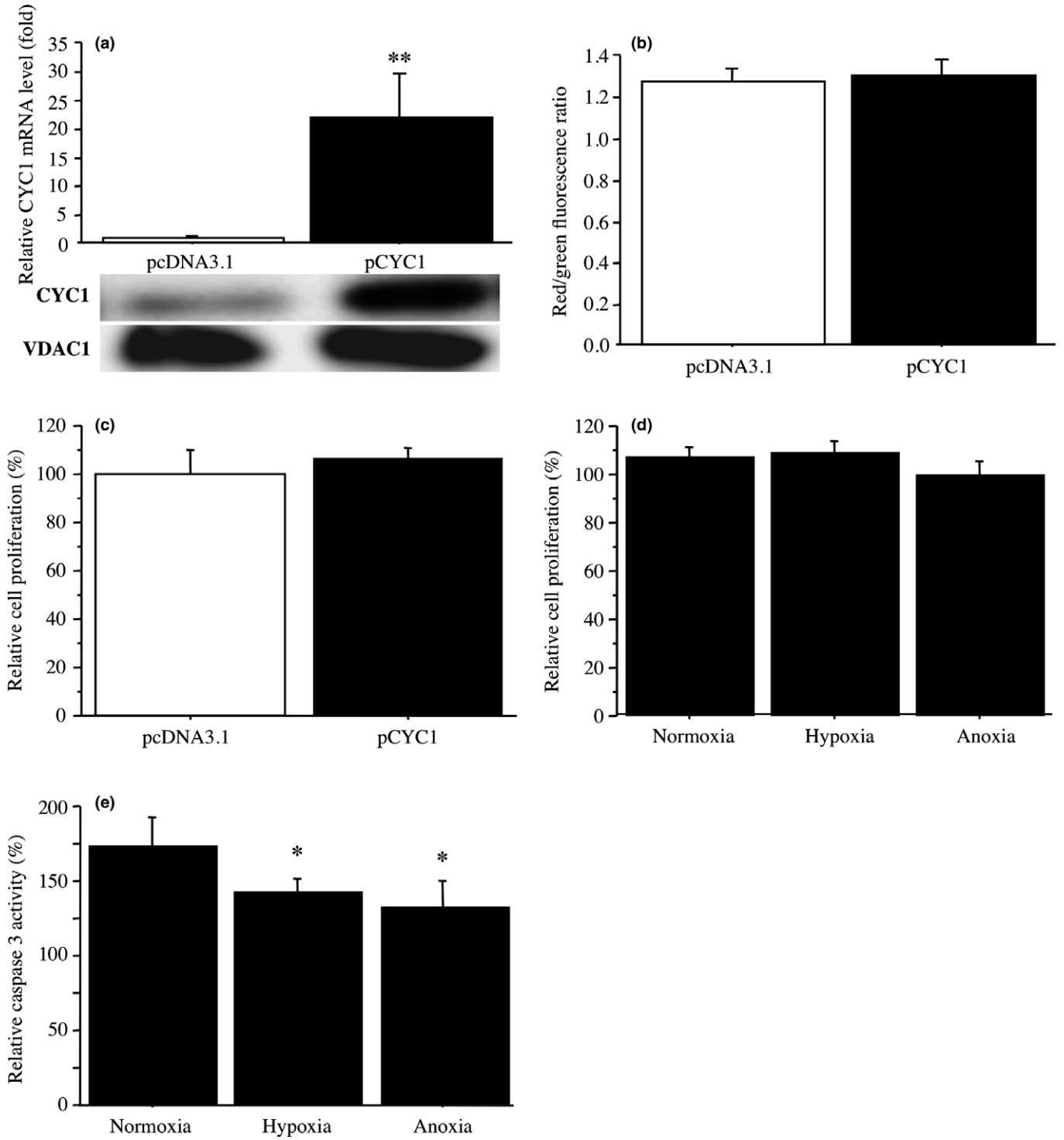

Fig. 5. Effects of cytochrome c1 (CYC1) overexpression on mitochondrial membrane potential, cell proliferation, and caspase 3 activity under hypoxia in MCF10DCIS.com ductal carcinoma *in situ* cells. (a) Upper panel, expression of CYC1 mRNA in MCF10DCIS.com cells transfected with CYC1 plasmid (pCYC1; closed bar) or control plasmid (pcDNA3.1; open bar) by real-time PCR. Lower panel, corresponding CYC1 immunoreactivity by immunoblotting. (b) JC-1 assays in MCF10DCIS.com cells transfected with CYC1 plasmid (closed bar) or control plasmid (open bar). Mitochondrial membrane potential was evaluated by red/green fluorescence ratio. (c) WST-8 assay in MCF10DCIS.com cells transfected with CYC1 plasmid (closed bar). Relative proliferative activity of these cells was summarized as a ratio (%) compared to control cells transfected with control plasmid (closed bar) at 2 days after treatment. (d) WST-8 assay in MCF10DCIS.com cells transfected with CYC1 plasmid under normoxia, hypoxia, or anoxia for 2 days. Relative cell proliferation activity was evaluated as a ratio (%) compared to the mean value of control cells transfected with control plasmid under the same condition. (e) Caspase 3 activity assays in MCF10DCIS.com cells transfected with CYC1 plasmid under normoxia, hypoxia, or anoxia for 5 h. Relative caspase 3 activity was evaluated as a ratio (%) compared to the mean value of control cells transfected with control plasmid under the same conditions. Data are presented as mean ± SD (n = 3). Statistical analyses were carried out using Fisher's PLSD test. *P < 0.05; **P < 0.01 versus left bar.

contribution of OXPHOS to the total cellular energy was 80% in MCF-7 breast carcinoma cells.[36] It is also true that the sensitivity of glucose-based PET is much lower for detecting DCIS than invasive breast cancer.[37]

In our present *in vitro* study, MCF10DCIS.com cells transfected with siRNA against CYC1 significantly decreased pro-apoptotic caspase 3 activity under anaerobic conditions compared to normoxia. Mitochondrial OXPHOS also regulates apoptosis and enhanced OXPHOS function increased intracellular oxidative stress and apoptosis.[35,38,39] Ducts in DCIS are frequently enlarged beyond 200 μm in diameter, although diffusion of oxygen from periductal vessels into ducts is limited to 100 μm, suggesting that the center of DCIS becomes poorly oxygenated.[24] Taken together with these previous findings and our present results, mitochondrial OXPHOS is suggested to play an important role in energy production of DCIS, at the early stages of breast carcinoma, and elevated OXPHOS activity through CYC1 overexpression might cause both increased proliferation activity and central comedo necrosis in DCIS. We could not examine the effects of CYC1 on formation of comedo necrosis in DCIS cells using a mouse transplantation model in this study, and further investigations are required.

In summary, we examined gene expression profiles of comedo DCIS using microarray analysis and showed that CYC1 is associated with comedo necrosis. CYC1 immunoreactivity was detected in 40% of DCIS cases, and it was associated with tumor size, nuclear grade, comedo necrosis, van Nuys classification, and Ki-67 LI. *In vitro* studies indicated that CYC1 was associated with mitochondrial membrane potential, increased proliferation activity, and increased pro-apoptotic caspase 3 activity under hypoxia. These results suggest that CYC1 plays an important role in cell proliferation and comedo necrosis by increasing OXPHOS activity in human DCIS.

Disclosure Statement

The authors have no conflict of interest.

Abbreviations

CYC1	cytochrome c1
DCIS	ductal carcinoma *in situ*
ER	estrogen receptor
GO	gene ontology
HER2	human epidermal growth factor receptor 2
LI	labeling index
OXPHOS	oxidative phosphorylation
PR	progesterone receptor
RPL13A	ribosomal protein L13A
siCTRL	negative control siRNA

References

1 American Cancer Society. Cancer Facts & Figures 2015. Atlanta: American Cancer Society 2015. Available from URL: http://www.cancer.org/acs/groups/content/@editorial/documents/document/acspc-044552.pdf.
2 Erbas B, Provenzano E, Armes J, Gertig D. The natural history of ductal carcinoma in situ of the breast: a review. *Breast Cancer Res Treat* 2006; **97**: 135–44.
3 Virnig BA, Wang SY, Shamilyan T, Kane RL, Tuttle TM. Ductal carcinoma in situ: risk factors and impact of screening. *J Natl Cancer Inst Monogr* 2010; **2010**: 113–16.
4 Meyer JS. Cell kinetics of histologic variants of in situ breast carcinoma. *Breast Cancer Res Treat* 1986; **7**: 171–80.
5 Lagios MD, Margolin FR, Westdahl PR, Rose MR. Mammographically detected duct carcinoma in situ. Frequency of local recurrence following tylectomy and prognostic effect of nuclear grade on local recurrence. *Cancer* 1989; **63**: 618–24.
6 Silverstein MJ, Poller DN, Waisman JR *et al.* Prognostic classification of breast ductal carcinoma-in-situ. *Lancet* 1995; **345**: 1154–7.
7 Pinder SE, Duggan C, Ellis IO, George WD; UK Coordinating Committee on Cancer Research (UKCCCR). Ductal Carcinoma In Situ (DCIS) Working Party. A new pathological system for grading DCIS with improved prediction of local recurrence: results from the UKCCCR/ANZ DCIS trial. *Br J Cancer* 2010; **103**: 94–100.
8 Yang Y, Karakhanova S, Hartwig W *et al.* Mitochondria and mitochondrial ROS in cancer: novel targets for anticancer therapy. *J Cell Physiol* 2016; **231**: 2570–81.
9 Fang W, Li X, Jiang Q *et al.* Transcriptional patterns, biomarkers and pathways characterizing nasopharyngeal carcinoma of Southern China. *J Transl Med* 2008; **6**: 32.
10 Li G, Fu D, Liang W *et al.* CYC1 silencing sensitizes osteosarcoma cells to TRAIL-induced apoptosis. *Cell Physiol Biochem* 2014; **34**: 2070–80.
11 Han Y, Sun S, Zhao M *et al.* CYC1 predicts poor prognosis in patients with breast cancer. *Dis Markers* 2016; **3528064**.
12 The Consensus Conference Committee. Consensus conference on the classification of ductal carcinoma in situ. *Cancer* 1997; **80**: 1798–802.
13 Ebata A, Suzuki T, Takagi K *et al.* Oestrogen-induced genes in ductal carcinoma in situ: their comparison with invasive ductal carcinoma. *Endocr Relat Cancer* 2012; **19**: 485–96.
14 Oka K, Suzuki T, Onodera Y *et al.* Nudix-type motif 2 in human breast carcinoma: a potent prognostic factor associated with cell proliferation. *Int J Cancer* 2011; **128**: 1770–82.
15 Sato-Tadano A, Suzuki T, Amari M *et al.* 2013 Hexokinase II in breast carcinoma: a potent prognostic factor associated with hypoxia-inducible factor-1α and Ki-67. *Cancer Sci* 2013; **104**: 1380–8.
16 Hammond ME, Hayes DF, Dowsett M *et al.* American Society of Clinical Oncology/College of American Pathologists guideline recommendations for immunohistochemical testing of estrogen and progesterone receptors in breast cancer (unabridged version). *Arch Pathol Lab Med* 2010; **134**: e48–72.
17 Miller FR, Santner SJ, Tait L, Dawson PJ. MCF10DCIS.com xenograft model of human comedo ductal carcinoma in situ. *J Natl Cancer Inst* 2000; **92**: 1185–6.
18 Behbod F, Kittrell FS, LaMarca H *et al.* An intraductal human-in-mouse transplantation model mimics the subtypes of ductal carcinoma in situ. *Breast Cancer Res* 2009; **11**: R66.
19 Grube S, Göttig T, Freitag D, Ewald C, Kalff R, Walter J. Selection of suitable reference genes for expression analysis in human glioma using RT-qPCR. *J Neurooncol* 2015; **123**: 35–42.
20 Clayton DA, Shadel GS. Isolation of mitochondria from tissue culture cells. *Cold Spring Harb Protoc* 2014; **10**: 1109–111. pdb.prot080002.
21 Zhu Y, Li M, Wang X *et al.* Caspase cleavage of cytochrome c1 disrupts mitochondrial function and enhances cytochrome c release. *Cell Res* 2012; **22**: 127–41.
22 Suzuki S, Takagi K, Miki Y *et al.* Nucleobindin 2 in human breast carcinoma as a potent prognostic factor. *Cancer Sci* 2012; **103**: 136–43.
23 Kong M, Ba M, Liang H, Shao P, Yu T, Wang Y. Regulation of adenosine triphosphate-sensitive potassium channels suppresses the toxic effects of amyloid-beta peptide (25–35). *Neural Regen Res* 2013; **8**: 56–63.
24 Bussolati G, Bongiovanni M, Cassoni P, Sapino A. Assessment of necrosis and hypoxia in ductal carcinoma in situ of the breast: basis for a new classification. *Virchows Arch* 2000; **437**: 360–4.
25 Muggerud AA, Hallett M, Johnsen H *et al.* Molecular diversity in ductal carcinoma in situ (DCIS) and early invasive breast cancer. *Mol Oncol* 2010; **4**: 357–68.
26 Vegfors J, Petersson S, Kovács A, Polyak K, Enerbäck C. The expression of Psoriasin (S100A7) and CD24 is linked and related to the differentiation of mammary epithelial cells. *PLoS One* 2012; **7**: e53119.
27 Emberley ED, Murphy LC, Watson PH. S100A7 and the progression of breast cancer. *Breast Cancer Res* 2004; **6**: 153–9.
28 Petersson S, Bylander A, Yhr M, Enerbäck C. S100A7 (Psoriasin), highly expressed in ductal carcinoma in situ (DCIS), is regulated by IFN-gamma in mammary epithelial cells. *BMC Cancer* 2007; **7**: 205.
29 Yin C, Li H, Zhang B *et al.* RAGE-binding S100A8/A9 promotes the migration and invasion of human breast cancer cells through actin polymerization and epithelial-mesenchymal transition. *Breast Cancer Res Treat* 2013; **14**: 297–309.
30 Martens C, Krett B, Laybourn PJ. 2001 RNA polymerase II and TBP occupy the repressed CYC1 promoter. *Mol Microbiol* 2001; **40**: 1009–19.
31 Ivanova MM, Luken KH, Zimmer AS *et al.* Tamoxifen increases nuclear respiratory factor 1 transcription by activating estrogen receptor beta and AP-1 recruitment to adjacent promoter binding sites. *FASEB J* 2011; **25**: 1402–16.

32 de Azambuja E, Cardoso F, de Castro G *et al.* Ki-67 as prognostic marker in early breast cancer: a meta-analysis of published studies involving 12,155 patients. *Br J Cancer* 2007; **96**: 1504–13.
33 Owens KM, Kulawiec M, Desouki MM, Vanniarajan A, Singh KK. Impaired OXPHOS complex III in breast cancer. *PLoS One* 2011; **6**: e23846.
34 Warburg O. On the origin of cancer cells. *Science* 1956; **123**: 309–14.
35 Księżakowska-Łakoma K, Żyła M, Wilczyński JR. Mitochondrial dysfunction in cancer. *Prz Menopauzalny* 2014; **13**: 136–44.
36 Guppy M, Leedman P, Zu X, Russell V. Contribution by different fuels and metabolic pathways to the total ATP turnover of proliferating MCF-7 breast cancer cells. *Biochem J* 2002; **364**: 309–15.
37 Azuma A, Tozaki M, Ito K, Fukuma E, Tanaka T, O'uchi T. Ductal carcinoma in situ: correlation between FDG-PET/CT and histopathology. *Radiat Med* 2008; **26**: 488–93.
38 Dey R, Moraes CT. Lack of oxidative phosphorylation and low mitochondrial membrane potential decrease susceptibility to apoptosis and do not modulate the protective effect of Bcl-x(L) in osteosarcoma cells. *J Biol Chem* 2000; **275**: 7087–94.
39 Yadav N, Kumar S, Marlowe T *et al.* Oxidative phosphorylation-dependent regulation of cancer cell apoptosis in response to anticancer agents. *Cell Death Dis* 2015; **6**: e1969.

Supporting Information

Additional Supporting Information may be found online in the supporting information tab for this article:

Table S1. Definition of enriched gene ontology terms in comedo ductal carcinoma *in situ* cases.

Table S2. Brief functions of genes listed in Table 1.